1
2

Standing genetic variation of the *AvrPm17* avirulence gene in powdery mildew limits the effectiveness of an introgressed rye resistance gene in wheat

5

Marion C. Mueller†[1], Lukas Kunz†[1], Seraina Schudel[1], Sandrine Kammerecker[1], Jonatan Isaksson[1], Michele Wyler[1], Johannes Graf[1], Alexandros G. Sotiropoulos[1], Coraline R. Praz[1], Thomas Wicker[1], Salim Bourras*[1, 2], Beat Keller*[1]

[1]Department of Plant and Microbial Biology, University of Zurich, Zurich, Switzerland
[2]Department of Forest Mycology and Plant Pathology, Division of Plant Pathology, Swedish University of Agricultural Sciences, Uppsala, Sweden

† Authors contributed equally

* Corresponding authors: Beat Keller, Salim Bourras

Email: bkeller@botinst.uzh.ch, salim.bourras@slu.se

15

16

Keywords

wheat, powdery mildew, resistance introgression, gene conversion, avirulence gene

19

Author Contributions

M.C.M., L.K., S.B. and B.K. wrote the paper. S.B., and B.K. coordinated the research. M.C.M., L.K., S.B. and B.K. designed the research. M.C.M. and S.S. performed genetic analysis. M.C.M., L.K., S.S. S.K. J.I. performed experiments. M.C.M, S.S., M.W., C.R.P. A.G.S, J.G. and T.W. performed bioinformatics analysis.

This PDF file includes:

Main Text
Figures 1 to 5

28

Abstract

Introgressions of chromosomal segments from related species into wheat are important sources of resistance against fungal diseases. The durability and effectiveness of introgressed resistance genes upon agricultural deployment is highly variable - a phenomenon that remains poorly understood as the corresponding fungal avirulence genes are largely unknown. Until its breakdown, the *Pm17* resistance gene introgressed from rye to wheat provided broad resistance against powdery mildew (*Blumeria graminis*). Here, we used QTL mapping to identify the corresponding wheat mildew avirulence effector *AvrPm17*. It is encoded by two paralogous genes that exhibit signatures of re-occurring gene conversion events and are members of a mildew sub-lineage specific effector cluster. Extensive haplovariant mining in wheat mildew and related sub-lineages identified several ancient virulent *AvrPm17* variants that were present as standing genetic variation in wheat powdery mildew prior to the *Pm17* introgression, thereby paving the way for the rapid breakdown of the *Pm17* resistance. QTL mapping in mildew identified a second genetic component likely corresponding to an additional resistance gene present on the 1AL.1RS translocation carrying *Pm17.* This gene remained previously undetected due to suppressed recombination within the introgressed rye chromosomal segment. We conclude that the initial effectiveness of 1AL.1RS was based on simultaneous introgression of two genetically linked resistance genes. Our results demonstrate the relevance of pathogen-based genetic approaches to disentangle complex resistance loci in wheat. We propose that identification and monitoring of avirulence gene diversity in pathogen populations becomes an integral part of introgression breeding to ensure effective and durable resistance in wheat.

Significance Statement

Domesticated and wild wheat relatives provide an important source of new immune receptors for wheat resistance breeding against fungal pathogens. The durability of these resistance genes is variable and difficult to predict, yet it is crucial for effective resistance breeding. We identified a fungal effector protein recognised by an immune receptor introgressed from rye to wheat. We found that variants of the effector allowing the fungus to overcome the resistance are ancient. They were already present in the wheat powdery mildew gene pool before the introgression of the immune receptor and are therefore responsible for the rapid resistance breakdown. Our study demonstrates that the effort to identify new resistance genes should be accompanied by studies of avirulence genes on the pathogen side.

62 **Main Text**

63

64 **Introduction**

65

66 Wheat is the most widely cultivated food crop and is susceptible to a number of fungal diseases.

67 For more than a century, breeding for genetically resistant cultivars that can durably withstand

68 disease has been one of the most important approaches for sustainable wheat production globally.

69 Introgressions of chromosomal segments from closely related wild grasses such as *Aegilops* or

70 *Agropyron* species (1, 2) and other crop species such as rye (*Secale cereale*) have been highly

71 valuable sources of new resistance gene specificities (3). Specifically, the 1BL.1RS or 1AL.1RS

72 translocations of the rye chromosome 1R introgressed into hexaploid (AABBDD) wheat (reviewed

73 in (4)) were of great relevance for wheat resistance breeding. Genes present on these

74 translocations are widely used in wheat breeding and confer resistance to leaf rust (*Lr26*), stripe

75 rust (*Yr9*), stem rust (*Sr31*, *Sr50/SrR, Sr1R^{Amigo}*) and powdery mildew (the allelic *Pm8*/*Pm17* pair),

76 (5, 6).

77 It has been proposed that introgressed resistance genes provide more effective and potentially

78 more durable resistance since pathogens specialized on wheat have previously not been exposed

79 and therefore have not adapted to the resistance specificities that evolved in other species (7). This

80 is exemplified by the rye *Sr31* gene, which was deployed worldwide. It provided effective and broad

81 resistance against *Puccinia graminis* f. sp. *tritici* the causal agent of wheat stem rust for over 30

82 years before being overcome by the virulent African strain Ug99 (8), demonstrating both the huge

83 benefit of an introgressed rye gene as well as the constant need for new broadly active resistance

84 genes (9). In contrast to *Sr31* and the general hypothesis, many introgressed resistance genes

85 were overcome quickly by wheat pathogens (10). For example, the rye introgressions with *Pm8*

86 and *Pm17* became ineffective against wheat powdery mildew *Blumeria graminis f. sp. tritici* (*B.g.*

87 *tritici*) within a few years after their deployment in large-scale agricultural settings (11-14). Thus, it

88 remains one of the most pressing questions in the field of plant breeding research why a few

89 introgressed genes such as *Sr31* remained effective over a long timeframe and despite worldwide

90 deployment whereas others are overcome quickly (7).

91 The allelic *Pm8* and *Pm17* genes encode for nucleotide-binding leucine rich repeat (NLR) proteins

92 that were introgressed into wheat from 'Petkus' and 'Insave' rye cultivars respectively (15, 16). It

93 was demonstrated that both genes represent rye homologs of the wheat *Pm3* resistance gene (15,

94 16) which encodes for a high number of different NLR alleles that confer race-specific resistance

95 against wheat powdery mildew through recognition of mildew encoded avirulence proteins (17-19).

96 In wheat powdery mildew recent studies using map-based cloning, GWAS and effector

97 benchmarking approaches have identified several avirulence genes, among them *AvrPm3$^{a2/f2}$*,

3

98   *AvrPm3^(b2/c2)* and *AvrPm3^(d3)* recognized by *Pm3a/Pm3f*, *Pm3b/Pm3c* and *Pm3d* respectively (17,
99   18). Sequence analysis of wheat mildew *Avr* genes revealed that they all encode small secreted
100   candidate effector proteins (17, 18, 20, 21) and exhibit high levels of sequence variation on a
101   population level including the independent evolution of numerous gain of virulence alleles by
102   diverse molecular mechanisms (17, 18, 20, 22). The identification and functional characterization
103   of mildew avirulence genes has therefore significantly broadened our understanding of race-
104   specific resistance and resistance gene breakdown in the wheat – mildew pathosystem.

105   Grass powdery mildews exist in many sub-lineages also called *formae speciales* (*f.sp.*) that are
106   highly host specific such as mildew on wheat (*B.g. tritici*), rye (*B. g. secalis*) or the wheat/rye hybrid
107   triticale (*B.g. triticale*) which emerged recently and was attributed to a hybridization event between
108   wheat and rye mildew sub-lineages (23, 24). Due to the strict host barrier, it is assumed that non-
109   adapted mildew sub-lineages have not been exposed to NLR resistance specificities of an
110   incompatible host and therefore have not evolved to evade recognition. Indeed, several *Pm3* alleles
111   have been found to contribute to non-host resistance through recognition of conserved avirulence
112   effectors in non-adapted mildew sub-lineages such as *B.g. secalis* (18). Given these observations,
113   the rapid breakdown of *Pm8* and *Pm17* resistance after introgression into wheat remains puzzling
114   and provides an opportunity to study evolutionary dynamics of wheat mildew in the context of
115   introgression breeding. The *Pm17* introgression is especially suited for this purpose since the
116   associated 1AL.1RS translocation, first described in 1976 in Oklahoma (US) (25), was not used
117   before the end of the 20th and has been deployed in large-scale agricultural setting only in the
118   beginning of the 21th century in the United States, where it provided resistance against wheat
119   mildew in bread wheat (26, 27). In contrast, the deployment in other wheat growing areas globally
120   started only after the year 2000 (11, 27-29), and breakdown of *Pm17* resistance was generally
121   observed within few years and has been well documented in several wheat growing regions such
122   as the US, China and Switzerland (11, 13, 27, 30).

123   In this study we report the molecular basis underlying the resistance breakdown of the introgressed
124   *Pm17* gene in wheat. Using QTL mapping in a bi-parental mildew population we demonstrate that
125   the corresponding avirulence effector *AvrPm17* is encoded by a paralogous effector gene pair,
126   residing in a dynamic effector cluster, specific to the wheat and rye mildew sub-lineages. Moreover,
127   we describe the identification of numerous ancient virulence alleles of the *AvrPm17* gene that have
128   been present as standing genetic variation in *B.g. tritici* even before the introgression of *Pm17* into
129   the wheat breeding pool. Lastly, we provide genetic evidence for the existence of a so far
130   unidentified resistance gene against wheat mildew which was co-introgressed with *Pm17* from rye,
131   which could be revealed through careful dissection of resistance specificities based on genetic
132   studies in the pathogen.

4

133 **Results**

134

135 ***QTL mapping identifies a single avirulence locus for Pm17 in wheat powdery mildew***

136 To understand the breakdown of the rye NLR *Pm17* in wheat we aimed at identifying its

137 corresponding avirulence gene by taking advantage of the recent cloning of *Pm17* and its validation

138 in transgenic wheat lines (16). We used a preexisting, sequenced F1 mapping population derived

139 from a cross of the avirulent *B.g. triticale* isolate THUN-12 and *B.g. tritici* isolate Bgt_96224 which

140 exhibits a virulent phenotype on the independent transgenic lines Pm17#34 and Pm17#181 (Fig.

141 S1A,B), (31). A single interval QTL mapping approach using 55 randomly selected progeny of the

142 Bgt_96224 X THUN-12 cross identified a single locus on chromosome 1 at identical map position

143 (164.8cM) with highly significant LOD scores of 9.2 for wheat genotype Pm17#34 and 7.0 for

144 Pm17#181 respectively (Fig. 1A-C, Fig S1C,D, Table S1). The pericentromeric location of the

145 mapped *AvrPm17* locus contrasts with the location of previously identified wheat mildew avirulence

146 genes that tend to reside near the telomeric region or on the chromosome arms (Fig. 1B, Fig. S2,

147 (17, 18, 20)).

148 To identify *AvrPm17* candidate genes we analysed the physical region underlying the QTL (with a

149 confidence interval of 1.5 LOD) on chromosome 1 in the chromosome-scale assemblies of the

150 parental isolates Bgt_96224 and THUN-12 ((31), unpublished data). The genetic confidence

151 interval corresponded to a 61.8kb region in the assembly of THUN-12 and a much larger region of

152 114.3 kb in the assembly of Bgt_96224. This striking difference in size is explained by a large 50kb

153 deletion in the THUN-12 genome (Fig. 1D-F). The interval in the *Pm17* avirulent isolate THUN-12

154 encodes only encodes a paralogous effector gene pair *BgTH12-04537* and *BgTH12-04538* (Fig.

155 1E). The two effector genes encode for identical proteins that differ by two synonymous single

156 nucleotide polymorphisms (SNPs). The two gene copies are encoded by two inverted duplicated

157 segments of 2'300bp separated by a 4'769bp intergenic region (Fig. 1F). The corresponding gene

158 duplication is also present in the corresponding region of the virulent parent Bgt_96224. There, the

159 duplicated effector genes *Bgt-51729* and *Bgt-51731* are identical and each carries two amino acid

160 changes (A53V, R80S) compared to BgTH12-04537 and BgTH12-04538 respectively (Fig. 1D-E,

161 Fig. 2A, Fig. S3). The interval in the Bgt_96624 genome encodes an additional effector gene;

162 *BgtAcSP-31098* that lies within the 50kb deleted region in THUN-12. In the absence of additional

163 genes in the locus of the avirulent parent THUN-12 we predicted that *BgTH12-04537* and *BgTH12-*

164 *04538* encode for *AvrPm17*. Using RNA-seq data from the parental isolates we found that *BgTH12-*

165 *04537/BgTH12-04538* and *Bgt-51729/Bgt-51731* are highly expressed at early stages of infection

166 corresponding to the establishment of the haustorial feeding structure at 2dpi, reminiscent of other

167 wheat mildew *Avr* genes (Fig. S4 and S5). The *AvrPm17* candidates are not differentially expressed

.

168   (logFC<1.5, Fig. S4) therefore indicating that the amino acid polymorphisms observed between

169   Bgt_96224 and THUN-12 must account for the difference in phenotype.

170   A previous study found that the hybrid genome of *B.g. triticale* isolates consists of distinct genomic

171   segments inherited from either wheat or rye mildew (23). Due to the rye origin of the *Pm17*

172   resistance gene, the origin of the avirulence locus in triticale mildew THUN-12 is of special interest.

173   Following the approach of (23) based on the analysis of fixed polymorphism between wheat and

174   rye mildew, we found that the physical region underlying the *AvrPm17* QTL in THUN-12 is a

175   segment inherited from wheat mildew (Fig. S6A-C). This indicates that that the rye *Pm17* gene

176   recognises an avirulence component originating from the non-adapted wheat powdery mildew

177   donor and not from the adapted rye mildew, in the triticale mildew hybrid.

178

Functional validation of *AvrPm17*

180   To functionally validate *AvrPm17,* we transiently co-expressed the *BgTH12-04537/BgTH12-04537*

181   Avr candidate with *Pm17*-HA in *Nicotiana benthamiana* by *Agrobacterium tumefaciens* mediated

182   transient overexpression (18, 20). All effector constructs were expressed without the signal peptide

183   and codon-optimized for expression in *N. benthamiana* to ensure optimal translation *in planta*.

184   *BgTH12-04537/BgTH12-04538* elicited a strong hypersensitive response (HR) upon co-expression

185   with Pm17-HA but not when expressed alone, confirming that these paralogous effector genes are

186   *AvrPm17* (Fig. 2B,C). Co-expression of *AvrPm17_THUN12* with either the *Pm8* gene from rye or

187   the *Pm17* orthologues from wheat (*Pm3a-f*, *Pm3CS*) did not result in a hypersensitive response in

188   *N. benthamiana* (Fig. S7), demonstrating the specificity of *AvrPm17_THUN-12* recognition by

189   *Pm17*.

190   Interestingly-co-expression of *AvrPm17_96224* with *Pm17*, also resulted in a hypersensitive

191   response. The extent of cell-death was however significantly reduced compared to the

192   *AvrPm17_THUN12* variant (paired Wilcoxon rank test p=0.0048) (Fig. 2D). We therefore concluded

193   that *Pm17* can weakly recognise *AvrPm17_96224*, at least in a heterologous overexpression

194   system. To address the question whether the weak recognition of *AvrPm17_96224* translates into

195   phenotypes on *Pm17* wheat we made use of the above-mentioned transgenic lines Pm17#181 and

196   Pm17#34 which were previously shown to exhibit differences in PM17 protein abundance with

197   Pm17#181 representing the stronger line (16). Consistent with a prediction of a quantitative

198   difference in AVR recognition, we observed reduced leaf coverage by mildew upon infection of the

199   strong line Pm17#181 with isolate 96224 and with progeny of the 96224 X THUN-12 cross carrying

200   the *AvrPm17_96224* haplotype (Fig. S1A-D), thus indicating that a residual recognition of

201   *AvrPm17_96224* by transgenic *Pm17* overexpression is sufficient to reduce disease severity

202 quantitatively. In contrast, the recognition of the *AvrPm17_THUN12* haplotype conferred complete

203 disease resistance in both transgenic lines (Fig. S1A,B,D). Taken together these findings

204 demonstrate that while the *Pm17* resistance in wheat genetically follows a classic gene-for-gene

205 interaction model, phenotypic differences in *Pm17* mediated resistance is not only determined by

206 sequence polymorphism in the AVR but also by Pm17 expression levels.

207 We therefore also analysed differences in AVR protein abundance using C-terminal FLAG epitope

208 tagged AVRPM17 variants from Bgt_96224 and THUN-12. The presence of the FLAG epitope

209 partially interfered with *AvrPm17* recognition since tagged versions exhibited significantly reduced

210 HR levels when co-expressed with *Pm17*, however the specificity was not affected (Fig. S8A-D).

211 Both AVRPM17-FLAG variants as well as PM17-HA were detectable on a Western blot (Fig. 2E,

212 Fig. S8E-F). Interestingly, expression of AVRPM17_THUN12 in *N. benthamiana* resulted in higher

213 protein abundance than for the weakly recognized AVRPM17-96224 variant (Fig. 2E). This

214 suggests that the amino acid polymorphisms between 96224 and THUN-12 affect protein stability

215 of AVRPM17 and therefore contribute to the differential recognition of the AVRPM17 variants by

216 PM17, thus further demonstrating that protein expression levels of AVR and NLR variants are

217 additional determinants underlying the seemingly binary gene-for-gene genetic determinism of

218 immunity based on major R genes. Similar observations were recently described for *AvrPm3*[a2/f2],

219 where polymorphism in the AVR were found to affect protein amount and thereby directly influence

220 recognition by *Pm3a* (32).

221 AVRPM17 is part of effector family E003, the second largest effector family found in *Blumeria*

222 *graminis* (31). The family is comprised of small proteins of c.a. 110 amino acids that contain a

223 predicted signal peptide, an N-terminal Y/FxC motif followed by a stretch of alternating hydrophobic

224 residues as well as a conserved carboxy-terminal cysteine (Fig. S9). These features have been

225 described for numerous *Blumeria* effectors, including all functionally characterized AVR proteins in

226 wheat mildew (18, 20, 21). Using an *in silico* modelling approach based on IntFOLD5.0, we found

227 that AVRPM17 is predicted to exhibit a ribonuclease-fold (pvalue = 1.145E-4), consisting of a single

228 α-helix and three β-strands (Fig. S10A,B). A similar ribonuclease-fold was experimentally

229 determined by crystallization for the barley powdery mildew (*B.g. hordei*) effector BEC1054 (33)

230 and proposed for AVRA7, the avirulence gene of the barley NLR Mla7 (34). *Avra7* is part of the

231 *AvrPm17* gene family (E003) (Fig. S11), suggesting that the ribonuclease-fold is conserved within

232 the effector family. The particular arrangement of α-helix helix and β-strands has been predicted

233 for other AVR proteins in wheat mildew. Most importantly such a pattern was described for the

234 entire effector families E008, E018 and E034 encoding *AvrPm3*[a2/f2], *AvrPm3*[b2c2] and *AvrPm3*[d3]

235 respectively (18). We therefore hypothesize that *AvrPm17* and the *AvrPm3*'s encode for structurally

236 similar proteins, despite little similarity on the primary amino acid sequences (Fig. S12) suggest

237 that the wheat *Pm3* allelic series and its rye orthologue *Pm17* recognise structurally related
238 effectors.

AvrPm17 is encoded in a mildew sub-lineage specific effector cluster and exhibits signs of re-occurring gene conversion events

241 Candidate effector genes in wheat and barley powdery mildew have been grouped into 235 families
242 based on sequence similarity (31). *AvrPm17* belongs to family E003 which is represented with 69
243 members in *B.g. tritici* (isolate Bgt_96224), 70 members in *B.g. triticale* (isolate THUN-12) and 59
244 members in *B.g. hordei* (isolate *DH14*) ((31),(34)). E003 is physically organized in gene clusters
245 distributed over seven of the eleven chromosomes of wheat and triticale mildew (Fig. S11). Family
246 members encoded in the same chromosomal location form phylogenetically related clades,
247 consistent with the previously proposed expansion mechanism of effector genes through local
248 duplication ((22), Fig. S11). Interestingly, the *AvrPm17* clade is encoded in a gene cluster that
249 spans more than 1.3Mb on chromosome 1 and contains 7 and 8 members in triticale and wheat
250 mildew respectively, as well as a solitary family member on chromosome 8 (Fig. 3A,B). The locus
251 also harbours an additional effector cluster from family E011, consisting of eleven members, that
252 has expanded within the E003 cluster (Fig. 3B). To study the evolutionary history of the *AvrPm17*
253 clade, we identified the region corresponding to the *AvrPm17* cluster on scaffold_27 in barley
254 mildew isolate DH14 based on conserved syntenic flanking genes. Strikingly, the region in DH14
255 is only 200kb in size and harbours only two E003 family members of the *AvrPm17* clade as well as
256 a single effector from family E011 (Fig. 3B). This indicates both effector clades have been
257 significantly expanded in wheat mildew after the divergence from the barley mildew lineage (Fig.
258 3B). Using re-sequencing data from five rye mildew strains we could also show that rye mildew has
259 six out of the eight E003 family members in the clade, whereas it lacks most of the E011 genes
260 (Fig 3B), indicating that the E003 expansion has happened in a progenitor of rye/wheat mildew
261 whereas the E011 family expansion in this region is wheat mildew specific. Strikingly, rye mildew
262 does not encode for an *AvrPm17* gene, consistent with the virulent phenotype of the five rye mildew
263 isolates on the *Pm17*-donor line 'Insave' (Fig. S13). This suggests that *AvrPm17* was lost in rye
264 mildew likely due to the selection pressure imposed by the *Pm17* gene in the rye gene pool.

265 Given the highly dynamic genomic context of the *AvrPm17* locus, it is striking that the avirulent
266 AVRPM17_THUN12 variant and the partial gain-of-virulence variant AVPM17_96224 are encoded
267 by near identical (*BgTH12-04537/BgTH12-04538,* two synonymous SNPs*)* or identical (*Bgt-51729/*
268 *Bgt-51731)* paralogous gene copies within the isolates THUN-12 and 96224, respectively (Fig.
269 S14). Most importantly, the three non-synonymous SNPs that differentiate *AvrPm17_96224* from
270 the avirulent *AvrPm17_THUN12* are identical in both genes *Bgt-51729 and Bgt-51731* (Fig. 3C).
271 Congruently there is an identical SNP in the intron of *Bgt-51729 and Bgt-51731*. It is highly unlikely

8

272 that the exact same four mutations have occurred independently in both genes, indicating a recent

273 gene duplication in each isolate. However, the duplicated region in Bgt_96224 and THUN-12 is

274 identical in size and position and therefore must have occurred in the ancestor of the two isolates

275 (Fig. 3C). Consistent with the hypothesis of a more ancient duplication event we found that flanking

276 regions of the duplication are significantly more divergent and contain two insertions (Fig. 3D/E,

277 Fig. S15,16, Supplementary Text 1). These findings further demonstrate that the duplication is older

278 than estimated based on the highly similar genic sequences. Therefore, the nucleotide

279 polymorphisms defining the differences between *AvrPm17_THUN12* and *AvrPm17_96224* have

280 most probably occurred in one gene copy and were then transferred to its duplicate by gene

281 conversion (for further details see Supplementary Text 1). We propose that gene conversion

282 event(s) contribute to the evolutionary potential of *AvrPm17* as an efficient way to transfer beneficial

283 mutations to both gene copies.

284 **Virulent *AvrPm17* haplovariants are ancient and predate *Pm17* introgression into wheat**

285 A haplotype mining approach in a diversity panel of 160 re-sequenced isolates of wheat mildew

286 (138) and triticale mildew (22 isolates) for *AvrPm17* revealed there are three dominant AVRPM17

287 variants in the gene pool (Fig. 4A,B). Two of these are the above-described AVPM17_THUN12

288 (varA) and the weakly recognized AVPM17_96224 (varB). The most frequent haplotype is varC

289 that contains a single amino acid polymorphism (A53V) and induces weaker HR in the *Nicotiana*

290 co-expression assays as compared to the functional varA found in THUN-12 (Fig. 4C). In addition,

291 eleven isolates originating from China encode for the only complete loss-of-recognition haplotype

292 found (varD) with three amino acid changes (A53V, E55R, G61A) compared to varA (Fig. 4A-C,

293 Fig. S17). Strikingly, 93% of the isolates with two *AvrPm17* copies encode for two identical mature

294 AVRPM17 proteins in one of the following combinations; varA/varA, varB/varB and varC/varC (Fig.

295 4B). This supports the hypothesis that the *AvrPm17* gene copies are kept identical by recurring

296 gene conversion events (for details see Supplementary Text 2, Fig. S14-16, S18-19, Table S2).

297 We selected a set of 16 representative isolates covering the diversity of *AvrPm17* in wheat mildew

298 (varA-varD), verified *AvrPm17* expression during early stages of infection (i.e. haustorial stage, Fig.

299 S20) and analyzed their virulence phenotype on *Pm17* transgenics. Consistent with the recognition

300 strength in *N. benthamiana*, representative isolates encoding for *AvrPm17_varD* were fully virulent

301 and isolates carrying *varA*, with the exception of one isolate, were avirulent on the transgenic *Pm17*

302 lines (Table S3). Isolates carrying the weakly recognized variants *AvrPm17_varB* and

303 *AvrPm17_varC* displayed intermediate phenotypes on the transgenic lines (Table S3). Thus, the

304 recognition strength of *AvrPm17* haplovariants observed in *N. benthamiana* largely correlated with

305 disease resistance in wheat thereby confirming the biological relevance of the heterologous

306 *Nicotiana* system to study quantitative effects of *Avr* recognition by resistance genes. Furthermore,

9

307   these findings indicate that *AvrPm17*_varD and *AvrPm17*_varB/varC indeed represent virulence or

308   partial virulence alleles respectively, that are likely responsible for the resistance breakdown of the

309   *Pm17* gene in wheat.

310   Both partially virulent variants varB and varC were present in all major subpopulations (i.e. China,

311   Europe, Israel, USA) (Fig. 4B). Given their global distribution and considering that some of the

312   isolates were collected already in the 1990's (SI appendix Dataset 3) this suggests that the partially

313   virulent *AvrPm17* variants varB and varC were present as standing genetic variation in the wheat

314   mildew population before large-scale agricultural deployment of wheat varieties carrying the *Pm17*

315   introgression at the beginning of the 21st century in the US, and only subsequently in other regions

316   of the world (27, 29). To further test this hypothesis, we extended our haplotype analysis to closely

317   related *formae speciales* of *B.g. tritici*. Due to their distinct host range*, B.g. dicocci*, a *forma specialis*

318   sampled on wild tetraploid wheat and *B.g. dactylidis* infecting the wild grass *Dactylidis glomerata*

319   (23, 35) are unlikely to have previously been exposed to the *Pm17* resistance gene. Strikingly, we

320   found that three isolates of *B.g. dicocci*, encode up to two copies of *AvrPm17_varB* (Fig. 4B).

321   Furthermore, we found three additional haplovariants (varE-G) specific to *B.g. diccoci*. Co-

322   expression of varE-G with *Pm17* in *N. benthamiana* resulted in significantly weaker HR responses

323   compared to *AvrPm17_varA*, indicating these variants also represent partially virulent alleles (Fig.

324   4C). This is consistent with the observation that these haplovariants share the A53V, R80S

325   mutation (varE,G) or the A53V mutation (varF) with AVRPM17_varB (Fig. 4A). Since *B.g. dicocci*

326   does not grow on most hexaploid wheat cultivars, including 'Bobwhite' (23) we could not test the

327   contribution of the varE-G recognition to *Pm17* virulence. In *B.g. dactylidis*, represented by two

328   isolates, we found an additional haplovariant *AvrPm17*_varBgd which carries two substitutions

329   *(*A53V and G61A) compared to *AvrPm17_varA* and is only very weakly recognized by *Pm17* in *N.*

330   *benthamiana* (Fig. 4A/C). Most importantly, these mutations are shared with the non-recognised

331   Chinese haplotype *AvrPm17_varD*, demonstrating that (i) the E55R substitution in the Chinese

332   haplotype is the causative mutation leading to complete loss-of-recognition by *Pm17* (Fig. 4C, Fig.

333   S17) and (ii) that part of the *AvrPm17* diversity found in wheat mildew is ancient and predates the

334   split of *B.g. tritici* and *B.g. dactylidis*. Taken together we found that a significant proportion of the

335   *AvrPm17* sequence diversity found in *B.g. tritici*, including several gain of virulence mutations, is

336   shared with its closely related *formae speciales B.g. dicocci* or *B.g. dactylidis.* Combined with the

337   observation of a global distribution of partially virulent *AvrPm17* variants B and C and their presence

338   in isolates collected before the deployment of *Pm17* wheat in agriculture, our findings strongly

339   indicate that these *AvrPm17* gain of virulence mutations represent standing genetic variation in

340   wheat mildew which predates precedes the introgression of *Pm17* into wheat.

341   While the existence of numerous virulent or partially virulent *AvrPm17* haplotypes in the global

342   mildew population prior to *Pm17* introgression might explain rapid *Pm17* resistance breakdown this

343   observation is hardly compatible with the initially described broad resistance phenotype exerted by

344   the 1AL.1RS translocation. Based on these considerations we therefore propose the 1AL.1RS

345   translocation to harbor a second mildew resistance gene in addition to *Pm17*.

346   **The 1RS.1AL translocation encodes for two powdery mildew resistance specificities**

347   To test for the predicted second resistance gene of the 1AL.1RS translocation, we characterized

348   the genetic association of avirulence of the 96224 X THUN-12 mapping population on the original

349   1AL.1RS translocation line 'Amigo' (16). The *Pm17* avirulent isolate THUN-12 showed an

350   intermediate phenotype on 'Amigo', demonstrating that recognition of *AvrPm17_varA* results in

351   quantitative resistance in presence of the endogenous *Pm17* gene (Fig. 5A,B). In contrast, the

352   *Pm17*-virulent isolate 96224 was avirulent on 'Amigo', indicating that (i) this isolate carries an

353   additional avirulence component recognized by 'Amigo' and (ii) the 96224 X THUN-12 bi-parental

354   population is suited to validate the second resistance specificity in 'Amigo' (Fig. 5C). Consistent

355   with our hypothesis, a QTL mapping analysis based on 117 progeny of Bgt_96224 X THUN12

356   identified two significant QTLs associated with the avirulence phenotype on cultivar 'Amigo' (for

357   details see Supplementary Text 3, Fig 5D, Table S4). One QTL on chromosome 1 corresponds to

358   the *AvrPm17* locus thereby verifying the activity of the *Pm17* gene in the original translocation line

359   'Amigo'. In addition, we identified a highly significant QTL on chromosome 9 that was not detected

360   in the QTL analysis on the transgenic *Pm17* lines (Fig. 1A, Fig. 5D), likely encoding the avirulence

361   component recognized by the predicted second resistance gene of the 1AL.1RS translocation. The

362   confidence interval of the QTL on chromosome 9 encompasses 371 kb in the avirulent isolate

363   96224 and harbors a total of 16 effector genes of which four are polymorphic compared to THUN-

364   12 (Table S5, Fig. S21A). Upon co-expression with *Pm17* in *N. benthamiana* none of the effector

365   candidates encoded by isolate Bgt_96224 within the confidence interval elicited a hypersensitive

366   response (Fig. S21B). This finding demonstrate that the second QTL on chromosome 9 is

367   independent of the *Pm17* resistance specificity. Most importantly, only progeny of the cross that

368   carry the *AvrPm17_96224* haplovariant (*AvrPm17_varB*) and the THUN-12 genotype in the QTL

369   on chromosome 9 are fully virulent (Fig. 5D,5E), further demonstrating that the simultaneous

370   presence of both virulence alleles is necessary to overcome the resistance on 'Amigo'.

371   We therefore conclude that the broad effectiveness of the 1AL.1RS translocation in providing

372   resistance against wheat powdery mildew was based on two resistance gene specificities in the

373   1AL.1RS translocation. Since the *Pm17* resistance specificity has been attributed to a single locus

374   based on segregation analysis we hypothesize that the second locus is genetically linked on the

375   1RS.1AL region and has previously been genetically masked due to repressed recombination

376   frequently associated with introgressed segments in wheat (36).

377   In summary, we here demonstrate that the *Pm17* introgression is genetically complex and that such

378   complexity could only be revealed through accurate genetic dissection of the avirulence

379   determinants in the pathogen distinguishing the two resistance specificities.

380

381 **Discussion**

382

383   The recent identification of numerous *Avr* genes both in *B.g. tritici* and *B.g. hordei* has significantly

384   advanced our understanding of NLR mediated resistance in the cereal powdery mildew

385   pathosystem (17, 18, 20-22, 34, 37). The functional cloning of *Avr* genes not only allowed

386   molecular studies on recognition mechanisms (32, 34) but has also set the ground for genetic

387   studies based on the natural diversity of avirulence components in local and global mildew

388   collections. This has led to the discovery of numerous gain of virulence mechanisms exerted by

389   *Blumeria* pathogens, including single amino acid polymorphisms, truncations and deletions of *Avr*

390   genes as well as a fungal encoded suppressor *SvrPm3* acting on *Pm3* mediated resistance

391   through masking of AVRPM3 recognition (17, 18, 34). These findings highlight the importance of

392   genetic and genomic studies in fungal plant pathogens in order to understand the mechanisms of

393   resistance breakdown and allow us to adapt current breeding approaches towards more durable

394   deployment of resistance genes in cereal crops.

395   With so far ten *Blumeria Avr* genes cloned and functionally characterized several patterns emerged.

396   *Blumeria* AVR effectors were found to be small proteins with a length of 102-130 amino acids, to

397   contain an N-terminal signal peptide, a largely conserved Y/FxC motif and a conserved cysteine

398   residue towards the C-terminus (17, 18, 20-22, 34, 37) while otherwise exhibiting highly divergent

399   amino acid sequences. Furthermore, wheat mildew *Avrs* were consistently among the highest

400   expressed genes within their effector gene family, indicating high abundance in host cells upon

401   secretion presumably influencing the efficacy of their virulence function alongside NLR mediated

402   recognition in resistant cultivars (18). The newly identified *AvrPm17* exhibits all the above-

403   mentioned characteristics of *Blumeria* AVRs and therefore further corroborates the emerging

404   patterns.

405   Despite showing little homology to proteins with a known function, more than a hundred *Blumeria*

406   effectors are predicted to exhibit a ribonuclease-like fold (20, 33, 34, 38, 39). Notably, such a

407   ribonuclease-like structure has recently been confirmed by protein crystallization of the barley

408   powdery mildew effector BEC1054 (33). Similarly, despite highly divergent amino acid sequences,

409   *in silico* protein modeling approaches predicted ribonuclease-like folds for most of the functionally

410   verified avirulence proteins in barley and wheat mildew (20, 21, 34), including all AVRPM3 effectors

411   (18) and AVRPM17 (this study). Based on the homology between rye *Pm17* and wheat *Pm3* NLRs

412   combined with the predicted structural similarities of their corresponding AVR proteins we propose

413   a conserved recognition mechanism, likely leading to similar selection pressures acting on AVR

414   genes for evasion of recognition.

415   Extensive haplovariant mining in a global wheat mildew collection for *AvrPm3*[a2/f2], *AvrPm3*[b2/c2] and

416   *AvrPm3*[d3] revealed that virulent alleles were exclusively based on single amino acid polymorphisms

13

417   (18, 22). Even though copy number variation was common, disruption or deletion of the avirulence

418   gene, as observed for many other *AVR*s has never been detected. In line with these findings, our

419   haplovariant mining approach for the paralogous *AvrPm17* copies in a comparable wheat mildew

420   diversity panel also failed to identify gene deletions or non-sense mutations and in return found

421   four variants varA-varD of which three represent partial or complete virulence alleles that are based

422   on amino acid polymorphisms. In contrast, we found the *AvrPm17* genes deleted in rye mildew,

423   suggesting different gain of virulence mechanisms in these closely related mildew sub-lineages,

424   likely due to differences in the exposure to the *Pm17* gene.

425   Gene duplications in effector genes are common and considered advantageous for pathogens as

426   they allow the independent diversification of virulence factors (31). However, the presence of

427   identical avirulence gene copies can represent a major liability as gain of virulence mutations need

428   to occur in both gene copies to effectively change the phenotypic outcome. This was described for

429   wheat mildew *AvrPm3^{d3}* in which gain of virulence mutations in one of the tandem duplicated gene

430   copies was not sufficient to render the isolates virulent (18). Gene conversion, efficiently

431   transferring beneficial mutations between gene copies, could provide pathogens with a molecular

432   mechanism to mitigate the disadvantage of duplicated avirulence genes. Indeed, a case of gene

433   conversion leading to gain of virulence was described for *Avr3c* in the oomycete *Phytophthora*

434   *sojae*, (40). Similarly, we found evidence for gene conversion to have occurred between the

435   paralogous copies of *AvrPm17* (Supplementary Text 1 & 2). The high frequency of wheat mildew

436   isolates encoding for varA/varA, varB/varB or varC/varC genotypes furthermore indicates repeated

437   gene conversion events between the two paralogs. Whether this phenomenon is dependent on

438   inherent predisposition of the locus to non-allelic gene conversion to occur or whether it reflects the

439   existence of an additional selection pressure linked to the virulence function of *AvrPm17* to maintain

440   the sequences identical will be subject to further studies.

441   It was hypothesized that introgressed *R* resistance genes provide effective and durable resistance

442   by recognizing an effector gene which, in the absence of previously acting diversifying selection, is

443   largely conserved (7). The opportunity to test this hypothesis for a fungal pathogen in wheat arose

444   with the recent cloning of the introgressed stem rust resistance genes *Sr35* (from *T. monococcum*,

445   (41)) and *Sr50* (from *Secale cereale*, (42)) and their corresponding avirulence genes *AvrSr35* and

446   *AvrSr50* in *Puccinia graminis* f. sp. *tritici (Pgt)* (43, 44). Virulent alleles for both genes were identified

447   in *Pgt* races with diverse geographic origins. Whether these virulent alleles emerged before the

448   introgression of *Sr35* and *Sr50* into wheat or as a consequence of their agricultural use was

449   however not assessed. The identification of partially or fully virulent *AvrPm17* haplovariants (varB-

450   varD) in a geographically diverse set of wheat mildew isolates collected over the last three decades

451   and the identification of *AvrPm17* homologs in closely related mildew sublineages provided a

14

452   unique opportunity to investigate a possible connection between the starting agricultural use of the
453   *Pm17* introgression in wheat at the beginning of the 21st century and the emergence of virulent
454   *AvrPm17* alleles in wheat mildew. Using (i) a global mildew population with a unique temporal
455   resolution including many isolates that were collected before *Pm17* deployment or exhibit different
456   host preferences (ii) careful phenotypic studies on transgenic *Pm17* lines, and (iii) functional studies
457   of *Avr* recognition in transient protein expression assays, we could demonstrate that virulent
458   *AvrPm17* variants were largely present in mildew populations prior to the deployment of *Pm17*. We
459   propose that this genetic diversity has arisen from the evolutionary arms-race between *Blumeria*
460   and its host species potentially tracing back to a Pm17/Pm3-like gene in the progenitor of rye and
461   wheat. This hypothesis is corroborated by the fact that the *AvrPm17* gene is encoded in a highly
462   expanded gene cluster of effector family E003, which is exclusive to wheat and rye mildew,
463   suggesting that the expansion of this cluster evolved prior to the split of the two mildew lineages
464   250'000 years ago (23). One of the mechanisms that is proposed to drive expansion of effector
465   gene clusters is the continuous coevolution with the host immune system (45, 46). Thus, the
466   presence of *Pm17/Pm3*-like genes in the progenitor of rye and wheat might have resulted in
467   selection pressure leading to the expansion of the effector cluster on chromosome 1 in the
468   progenitor of wheat and rye mildew, suggesting a long history of *R*-gene mediated effector evolution
469   in natural ecosystems, long before the start of agricultural cultivation. Our findings highlight the
470   importance for resistance durability to select introgressed resistance specificities based on the
471   evolutionary history of donor and recipient species. In this work, we demonstrate the necessity to
472   identify and monitor the genetic diversity of the corresponding avirulence factors in order to achieve
473   effective and durable resistance. We propose that such studies are very timely, considering the
474   current important efforts to introgress *R* genes into wheat from phylogenetically distant wild
475   relatives or phylogenetically close diploid progenitor species.

476   An often-stated advantage of larger translocations from related species is the simultaneous
477   introgression of several resistance specificities active against different plant pathogens such as the
478   most widely deployed rye translocation 1BL.1RS from 'Petkus' carrying *Lr26*, *Yr9*, *Sr31* and *Pm8*
479   (4). For effective and durable resistance, the introgression of several resistance genes active
480   against the same pathogen is highly desirable. By extending the mildew QTL mapping approach
481   from *Pm17* transgenic lines to the original 1RS.1AL translocation cultivar 'Amigo' we have found
482   evidence for the presence of a second resistance gene potentially recognizing an avirulence gene
483   of *B.g. tritici* isolate Bgt_96224. Historically the *Pm17* resistance associated with the 1RS.1AL
484   translocation has been attributed to a single locus (47). The additional resistance specificity
485   predicted by our QTL approach is therefore most likely genetically linked with the *Pm17* gene and
486   has been missed by genetic approaches solely applied on the plant side due to suppressed
487   recombination within the translocated genomic region originating from 'Insave' rye (36). The

15

488 simultaneous presence of two race-specific resistance genes in the 1RS.1AL translocation might

489 explain the initially broad resistance exhibited by cultivars such as 'Amigo', despite the likely long-

490 standing presence of several gain of virulence alleles for *AvrPm17* in the *B.g. tritici* population. The

491 identification of this second so far unknown AVR/R gene pair in the future will potentially provide

492 further answers regarding the initial efficacy but also the quick breakdown of the powdery mildew

493 resistance encoded on the 1RS.1AL translocation.

494 Identification and cloning of introgressed resistance genes has often been hampered by the

495 absence of recombination throughout parts or the entirety of the alien chromatin regions (48). In

496 recent years several technological advances such as RenSeq or MutChromSeq approaches that

497 do not rely on fine-mapping have helped to alleviate this phenomenon and led to the identification

498 of numerous new resistance genes often residing in highly complex loci (49, 50). Here we show

499 that genetic mapping populations of plant pathogens could provide an additional tool to dissect

500 complex translocated genomic regions with low or absent recombination thereby complementing

501 recently developed, plant-focused approaches.

502 **Materials and Methods**
503
504 Detailed Material and Methods section is available as SI appendix. Constructs used in this study

505 are listed in SI appendix Dataset 1. Primer sequences are listed in SI appendix Dataset 2. Details

506 about powdery mildew isolates and their associated (SRA) accession numbers are listed in SI

507 appendix Dataset 3. Phenotyping and subsequent QTL analysis are described in SI appendix

508 section 1. Candidate identification is described in SI appendix section 2 Construction of the

509 expression plasmids are described in SI appendix section 3. Transient expression procedure using

510 *Agrobacterium tumefaciens* in *Nicotiana benthamiana* followed by hypersensitive response

511 measurement are described in SI appendix section 4, western blot detection of tagged avirulence

512 and resistance genes can be found in SI appendix section 5. Expression analysis can be found in

513 Si appendix section 6. Bioinformatic analysis are detailed under 'SI appendix section 7. The

514 Sequence of *Pm17* is available at GeneBank under the accession number AYD60116.1. AvrPm17

515 haplovariants are available under the accession numbers XX-XX.

516
517 **Acknowledgments**
518

523
524

525 **References**
526

527 1.   P. Zhang *et al.*, "Wheat–Aegilops Introgressions In: Molnár-Láng M., Ceoloni C., Doležel
528   J. (eds) Alien Introgression in Wheat.". (Springer International Publishing, Cham, 2015),
529   pp. 221-243.
530 2.   C. Ceoloni, L. Kuzmanovic, P. Forte, M. E. Virili, A. Bitti, "Wheat-Perennial Triticeae
531   Introgressions: Major Achievements and Prospects   In: Molnár-Láng M., Ceoloni C.,
532   Doležel J.(eds) Alien Introgression in Wheat.". (Springer International Publishing, Cham,
533   2015), pp. 273-313.
534 3.   B. B. H. Wulff, M. J. Moscou, Strategies for transferring resistance into wheat: from wide
535   crosses to GM cassettes. *Frontiers in Plant Science* **5**, 11 (2014).
536 4.   L. A. Crespo-Herrera, L. Garkava-Gustavsson, I. Ahman, A systematic review of rye
537   (Secale cereale L.) as a source of resistance to pathogens and pests in wheat (Triticum
538   aestivum L.). *Hereditas* **154**, 1-9 (2017).
539 5.   B. Friebe, J. Jiang, W. J. Raupp, R. A. McIntosh, B. S. Gill, Characterization of wheat-alien
540   translocations conferring resistance to diseases and pests: Current status. *Euphytica* **91**,
541   59-87 (1996).
542 6.   R. Mago *et al.*, Identification and mapping of molecular markers linked to rust resistance
543   genes located on chromosome 1RS of rye using wheat-rye translocation lines.
544   *Theoretical and Applied Genetics* **104**, 1317-1324 (2002).
545 7.   J. G. Ellis, E. S. Lagudah, W. Spielmeyer, P. N. Dodds, The past, present and future of
546   breeding rust resistant wheat. *Frontiers in Plant Science* **5** (2014).
547 8.   Z. A. Pretorius, R. P. Singh, W. W. Wagoire, T. S. Payne, Detection of virulence to wheat
548   stem rust resistance gene Sr31 in Puccinia graminis. f. sp. tritici in Uganda. *Plant Disease*
549   **84**, 203-203 (2000).
550 9.   M. Ravensdale, A. Nemri, P. H. Thrall, J. G. Ellis, P. N. Dodds, Co-evolutionary
551   interactions between host resistance and pathogen effector genes in flax rust disease.
552   *Molecular Plant Pathology* **12**, 93-102 (2011).
553 10.   R. McIntosh, C. Wellings, R. Park, Wheat Rusts: An Atlas of Resistance Genes. *CSIRO*
554   *Publishing* (1995).
555 11.   C. Cowger, R. Parks, D. Marshall, Appearance of Powdery Mildew of Wheat Caused by
556   Blumeria graminis f. sp tritici on Pm17-Bearing Cultivars in North Carolina. *Plant Disease*
557   **93**, 1219-1219 (2009).
558 12.   C. Cowger, L. Mehra, C. Arellano, E. Meyers, J. P. Murphy, Virulence Differences in
559   Blumeria graminis f. sp tritici from the Central and Eastern United States.
560   *Phytopathology* **108**, 402-411 (2018).
561 13.   F.-s. Zeng *et al.*, Virulence and Diversity of Blumeria graminis f. sp. tritici Populations in
562   China. *Journal of Integrative Agriculture* **13**, 2424-2437 (2014).
563 14.   M. Heun, B. Friebe, Introgression of powdery mildew resistance from rye into wheat.
564   *Phytopathology* **80**, 242-245 (1990).
565 15.   S. Hurni *et al.*, Rye Pm8 and wheat Pm3 are orthologous genes and show evolutionary
566   conservation of resistance function against powdery mildew. *Plant Journal* **76**, 957-969
567   (2013).
568 16.   S. P. Singh *et al.*, Evolutionary divergence of the rye Pm17 and Pm8 resistance genes
569   reveals ancient diversity. *Plant Molecular Biology* **98**, 249-260 (2018).

570 17. S. Bourras *et al.*, Multiple Avirulence Loci and Allele-Specific Effector Recognition
571   Control the Pm3 Race-Specific Resistance of Wheat to Powdery Mildew. *Plant Cell* **27**,
572   2991-3012 (2015).
573 18. S. Bourras *et al.*, The AvrPm3-Pm3 effector-NLR interactions control both race-specific
574   resistance and host-specificity of cereal mildews on wheat. *Nature Communications* **10**,
575   2292 (2019).
576 19. S. Brunner *et al.*, Intragenic allele pyramiding combines different specificities of wheat
577   Pm3 resistance alleles. *Plant Journal* **64**, 433-445 (2010).
578 20. C. R. Praz *et al.*, AvrPm2 encodes an RNase-like avirulence effector which is conserved in
579   the two different specialized forms of wheat and rye powdery mildew fungus. *New*
580   *Phytologist* **213**, 1301-1314 (2017).
581 21. T. Hewitt *et al.*, A highly differentiated region of wheat chromosome 7AL encodes a
582   Pm1a immune receptor that recognises its corresponding AvrPm1a effector from
583   Blumeria graminis. *New Phytologist* **n/a** (2020).
584 22. K. E. McNally *et al.*, Distinct domains of the AVRPM3(A2/F2) avirulence protein from
585   wheat powdery mildew are involved in immune receptor recognition and putative
586   effector function. *New Phytologist* **218**, 681-695 (2018).
587 23. F. Menardo *et al.*, Hybridization of powdery mildew strains gives rise to pathogens on
588   novel agricultural crop species. *Nature Genetics* **48**, 201-205 (2016).
589 24. V. Troch, K. Audenaert, B. Bekaert, M. Hofte, G. Haesaert, Phylogeography and virulence
590   structure of the powdery mildew population on its 'new' host triticale. *Bmc Evolutionary*
591   *Biology* **12**, 76 (2012).
592 25. S. V. Rabinovich, Importance of wheat-rye translocations for breeding modern cultivars
593   of Triticum aestivum L. (Reprinted from Wheat: Prospects for global improvement,
594   1998). *Euphytica* **100**, 323-340 (1998).
595 26. R. Graybosch, G. Bai, P. S. Amand, G. Sarath, Persistence of rye (Secale cereale L.)
596   chromosome arm 1RS in wheat (Triticum aestivum L.) breeding programs of the Great
597   Plains of North America. **66**, 941-950 (2019).
598 27. R. Parks, I. Carbone, J. P. Murphy, D. Marshall, C. Cowger, Virulence structure of the
599   Eastern US wheat powdery mildew population. *Plant Disease* **92**, 1074-1082 (2008).
600 28. A. J. Lukaszewski, Frequency of 1RS.1AL and 1RS.1BL Translocations in United-States
601   Wheats. *Crop Science* **30**, 1151-1153 (1990).
602 29. A. J. Lukaszewski, "Introgressions Between Wheat and Rye In: Molnár-Láng M., Ceoloni
603   C.,Doležel J. (eds) Alien Introgression in Wheat.". (Springer International Publishing,
604   Cham, 2015), pp. 163-189.
605 30. F. Mascher *et al.* (2012) Virulenzmonitoring und Populationsstruktur des Echten
606   Mehltaus von 2003 bis 2010. (Agrarforschung Schweiz), pp 236–243.
607 31. M. C. Müller *et al.*, A chromosome-scale genome assembly reveals a highly dynamic
608   effector repertoire of wheat powdery mildew. *New Phytologist* **221**, 2176-2189 (2019).
609 32. S. Lindner *et al.*, Single residues in the LRR domain of the wheat PM3A immune receptor
610   can control the strength and the spectrum of the immune response. *Plant Journal*
611   (2020).
612 33. H. G. Pennington *et al.*, The fungal ribonuclease-like effector protein CSEP0064/BEC1054
613   represses plant immunity and interferes with degradation of host ribosomal RNA. *Plos*
614   *Pathogens* **15** (2019).
615 34. I. M. L. Saur *et al.*, Multiple pairs of allelic MLA immune receptor-powdery mildew
616   AVR(A) effectors argue for a direct recognition mechanism. *Elife* **8** (2019).

617 35. F. Menardo, T. Wicker, B. Keller, Reconstructing the Evolutionary History of Powdery
618   Mildew Lineages (Blumeria graminis) at Different Evolutionary Time Scales with NGS
619   Data. *Genome Biology and Evolution* **9**, 446-456 (2017).
620 36. E. L. Olson *et al.*, Genotyping of US Wheat Germplasm for Presence of Stem Rust
621   Resistance Genes Sr24, Sr36 and Sr1RS(Amigo). *Crop Science* **50**, 668-675 (2010).
622 37. X. L. Lu *et al.*, Allelic barley MLA immune receptors recognize sequence-unrelated
623   avirulence effectors of the powdery mildew pathogen. *Proceedings of the National
624   Academy of Sciences of the United States of America* **113**, E6486-E6495 (2016).
625 38. P. D. Spanu, Cereal immunity against powdery mildews targets RNase-Like Proteins
626   associated with Haustoria (RALPH) effectors evolved from a common ancestral gene.
627   *New Phytologist* **213**, 969-971 (2017).
628 39. C. Pliego *et al.*, Host-Induced Gene Silencing in Barley Powdery Mildew Reveals a Class
629   of Ribonuclease-Like Effectors. *Molecular Plant-Microbe Interactions* **26**, 633-642
630   (2013).
631 40. S. Dong *et al.*, The Phytophthora sojae Avirulence Locus Avr3c Encodes a Multi-Copy
632   RXLR Effector with Sequence Polymorphisms among Pathogen Strains. *Plos One* **4**
633   (2009).
634 41. C. Saintenac *et al.*, Identification of Wheat Gene Sr35 That Confers Resistance to Ug99
635   Stem Rust Race Group. *Science* **341**, 783-786 (2013).
636 42. R. Mago *et al.*, The wheat Sr50 gene reveals rich diversity at a cereal disease resistance
637   locus. *Nature Plants* **1** (2015).
638 43. J. P. Chen *et al.*, Loss of AvrSr50 by somatic exchange in stem rust leads to virulence for
639   Sr50 resistance in wheat. *Science* **358**, 1607-+ (2017).
640 44. A. Salcedo *et al.*, Variation in the AvrSr35 gene determines Sr35 resistance against
641   wheat stem rust race Ug99. *Science* **358**, 1604-1606 (2017).
642 45. A. Sanchez-Vallet *et al.*, The Genome Biology of Effector Gene Evolution in Filamentous
643   Plant Pathogens. LID - 10.1146/annurev-phyto-080516-035303 [doi]. (2018).
644 46. F. Menardo, C. R. Praz, T. Wicker, B. Keller, Rapid turnover of effectors in grass powdery
645   mildew (*Blumeria graminis*). *Bmc Evolutionary Biology* **17**, 223 (2017).
646 47. J. R. Lowry, D. J. Sammons, P. S. Baenziger, J. G. Moseman, Identification and
647   characterization of the gene conditioning powdery mildew resistance in Amigo wheat.
648   *Crop Science* **24**, 129-132 (1984).
649 48. D. H. Koo, W. X. Liu, B. Friebe, B. S. Gill, Homoeologous recombination in the presence of
650   Ph1 gene in wheat. *Chromosoma* **126**, 531-540 (2017).
651 49. J. Sanchez-Martin *et al.*, Rapid gene isolation in barley and wheat by mutant
652   chromosome sequencing. *Genome Biology* **17** (2016).
653 50. F. Jupe *et al.*, Resistance gene enrichment sequencing (RenSeq) enables reannotation of
654   the NB-LRR gene family from sequenced plant genomes and rapid mapping of resistance
655   loci in segregating populations. *Plant Journal* **76**, 530-544 (2013).

656
657

Figures and Tables
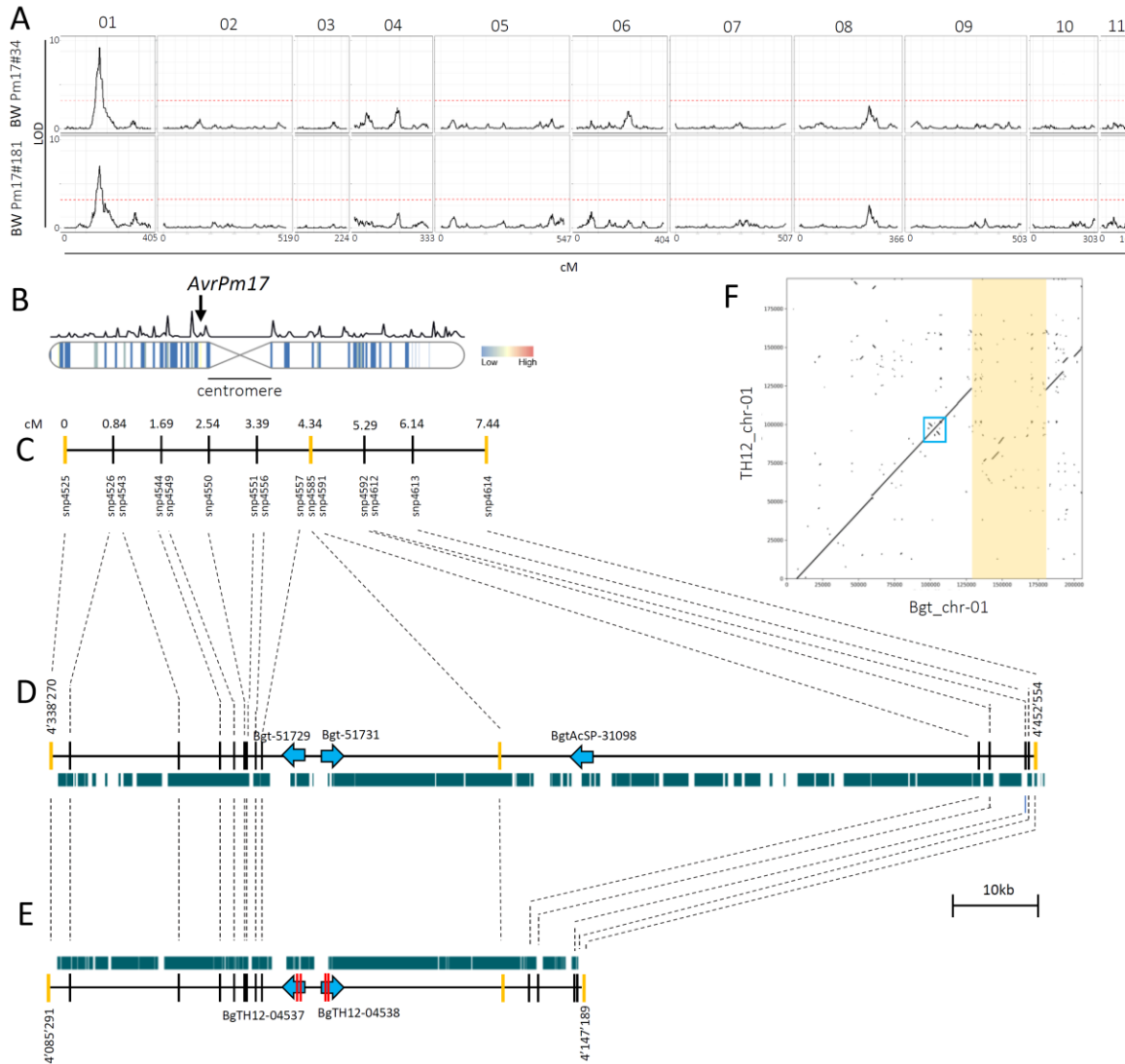
659
660 **Figure 1.** Avirulence on wheat genotypes with *Pm17* is controlled by a single locus in a biparental
661 mapping population between *B.g. tritici* 96224 X *B.g. triticale* THUN-12. (A) Single interval QTL
662 mapping of 55 progeny of the cross 96224X THUN-12 on two transgenic lines expressing *Pm17*-
663 HA under control of the maize ubiquitin promoter (Ubi) promoter. The genetic map of Bgt_96224 X
664 THUN-12 based on 119,023 markers was published previously in (31) and contains eleven linkage
665 groups that correspond to the eleven chromosomes of *B.g. tritici* 96224 and *B.g. triticale* THUN-12
666 ((31), unpublished data) Significance level of the LOD (logarithm of the odds) value was determined
667 using 1000 permutations and is indicated by a red line. (B) Location of the QTLs identified in the
668 pericentromeric region of chromosome 1 of *B.g. tritici* 96224. The centromeric region is indicated.
669 Vertical bars indicate effector gene density in 50kb windows following a gradient indicated in the
670 color key.. Line above the chromosome indicates the recombination rate in cM/50kb as described
671 in (31). The remaining ten chromosomes are depicted in Fig. S2. (C) Informative markers in the
672 7.44 cM genetic confidence interval (1.5LOD) and their cM position relative to the left flanking
673 marker. Flanking markers and the best associated marker of the QTL are depicted in yellow. (D-E)
674 Physical interval underlying the genetic interval in *B.g. tritici* 96224 (D) and *B.g. triticale* THUN12
675 (E). Gene and gene orientation are indicated with blue arrows (gene length not drawn to scale).
676 Non-synonymous SNPs in THUN-12 versus isolate 96224 are indicated by a red bar within the
677 gene. (D-E) Green bars indicates the presence of transposable elements in the interval. (F)

20

678   Alignment showing the region flanking 1Mb up and downstream of the *AvrPm17* locus in the
679   reference assemblies of *B.g. tritici* 96224 and *B.g. triticale* THUN-12. The location of the paralogous
680   effectors *BgTH12-04537*/*BgTH12-04538* and *Bgt-51729/Bgt-51731* is indicated by a blue box. The
681   50kb deletion in THUN-12 compared to 96224 is highlighted in yellow.
682
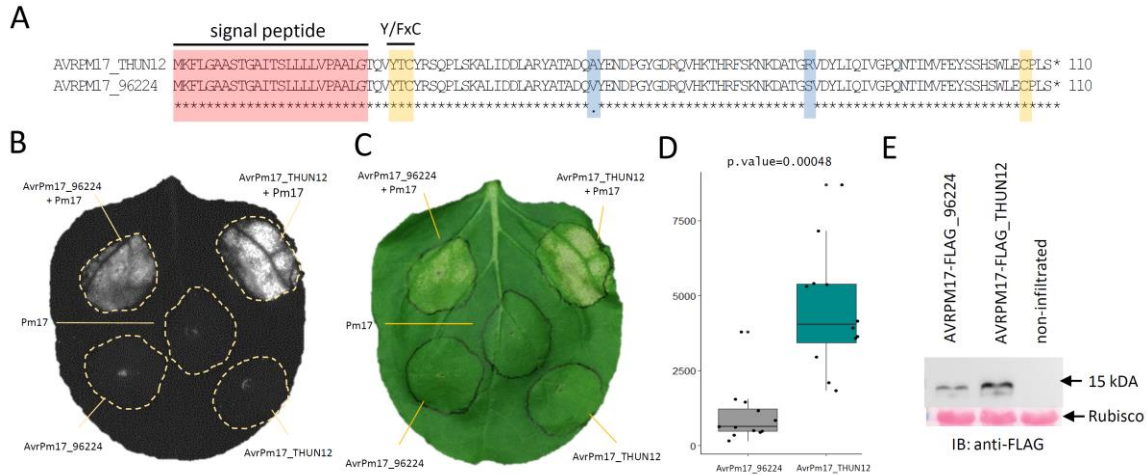
Figure 2. Functional validation of *AvrPm17* in *N. benthamiana* (A) Protein alignment of the AVRPM17 candidate in THUN-12 and 96224. Predicted signal peptide, Y/FxC motif and C-terminal cysteine residues are indicated in red and yellow, respectively. Polymorphic amino acid residues between Bgt_96224 and THUN-12 are highlighted in blue. (B-C) Co-expression of *Pm17*-HA and *AvrPm17*_THUN12 (*BgTH12-04537/BgTH12-04538*) and *AvrPm17*_96224 (*Bgt-51729/Bgt-51731*) by transient Agrobacterium-mediated expression in *Nicotiana benthamiana,* imaged by the Fusion FX imager system (B) or a conventional camera (C). Co-infiltrations were done at a ratio of 1:4 R:Avr. (D) Difference in hypersensitive response induction between the two AVRPM17 variants AVRPM17_THUN12 and AVRPM17_96224 infiltrated in a ratio of R:Avr of 1:1. The p-values of the paired Wilcoxon-ranked sum test is indicated above the panel. (E) Western blot showing C-terminal tagged AVRPM17-FLAG variants extracted from *A. tumefaciens* infiltrated leaf areas of *N. benthamiana* at 2dpi.
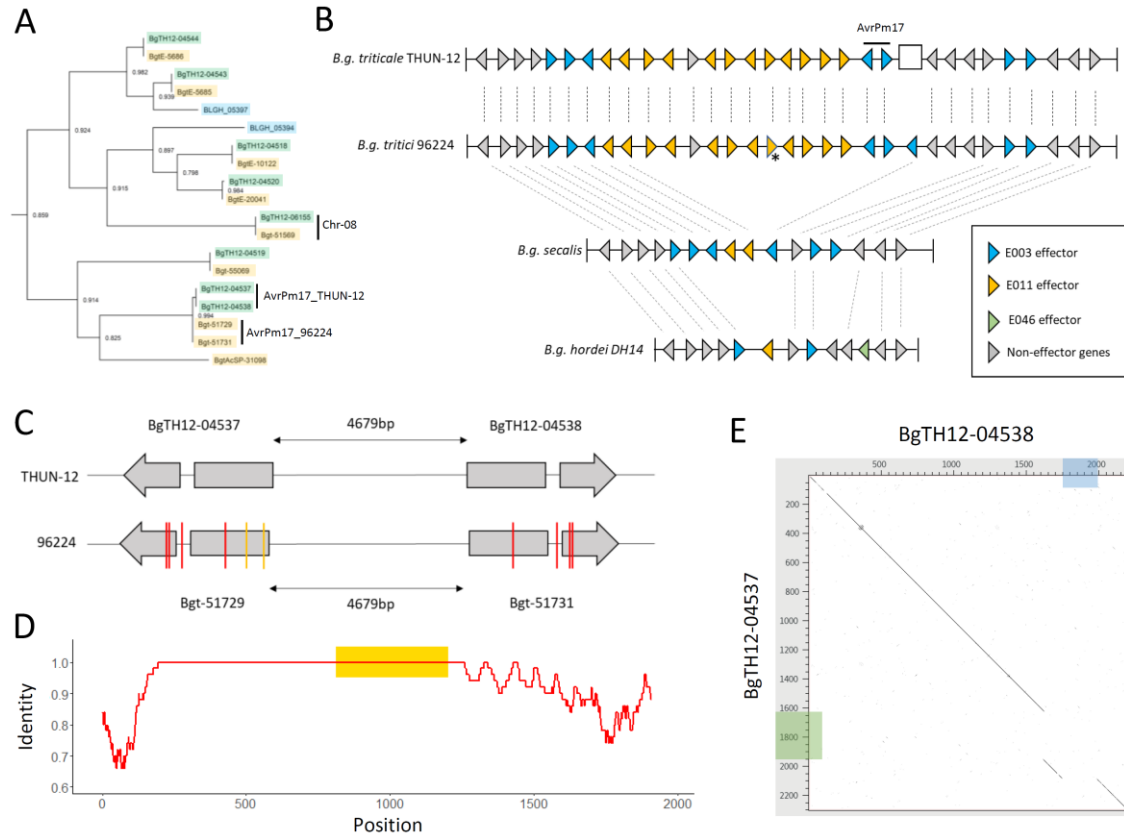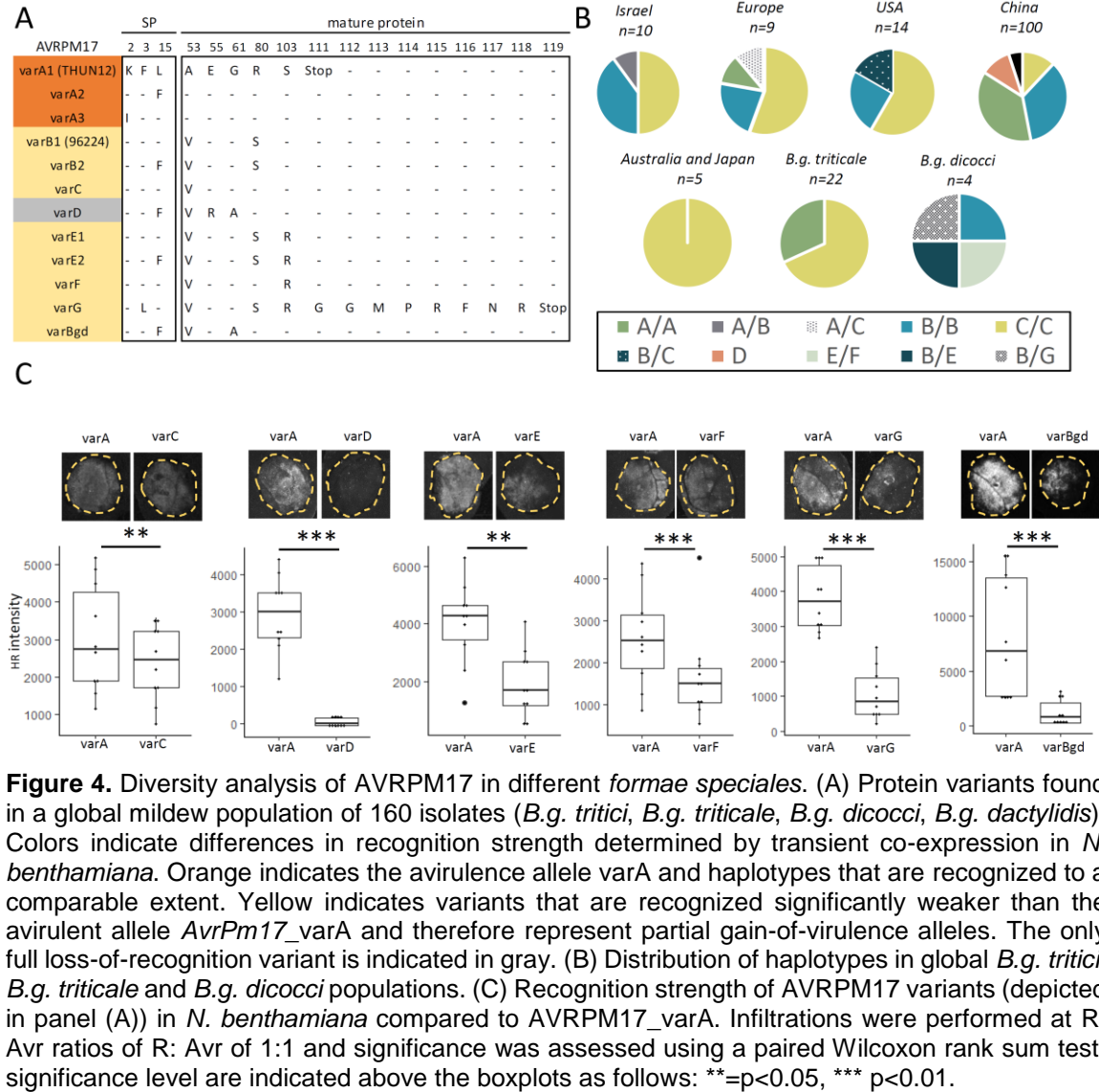
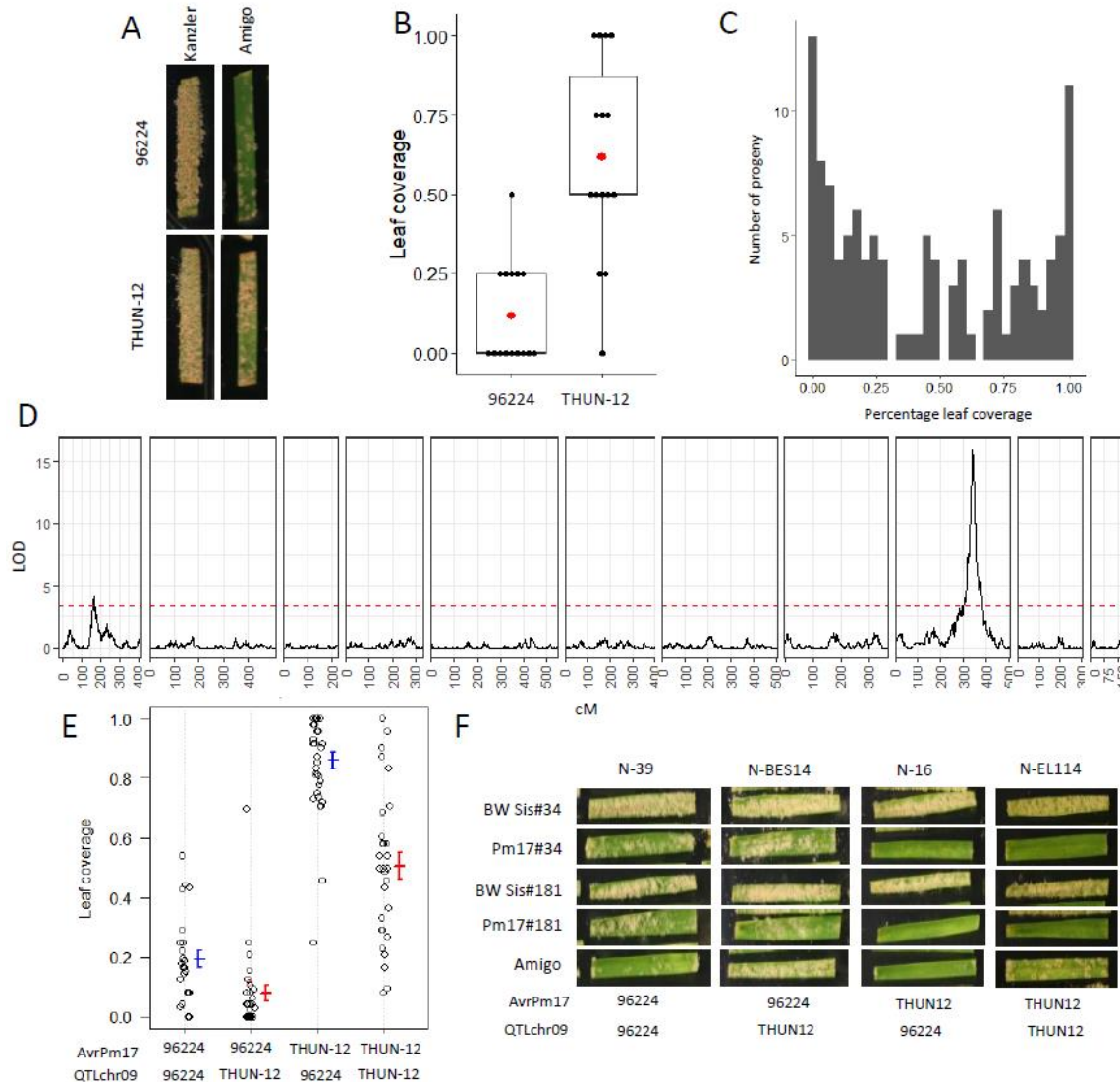**Figure 3.** *AvrPm17* is a member of a highly expanded effector gene cluster. (A) Phylogenic relationship of the AvrPm17 effector family. Panel shows subsection of the phylogenetic tree based on protein sequences of E003 effector family members of *B.g. tritici* (69 members) *B.g.* triticale (70 members) and *B.g. hordei* (59 members). The full tree can be found in Fig. S12. Effector family members are highlighted as follows: members in *B.g. tritici* in yellow, members in *B.g. triticale* in green, and members in *B.g. hordei* in blue. For each branch, the local support values calculated with the Shimodaira-Hasegawa test are indicated. (B) Schematic representation of the *AvrPm17* effector cluster in the high-quality genomes of *B.g. triticale* THUN-12, *B.g. tritici* 96224, and *B.g. hordei* DH14. In the absence of a high-quality genome assembly for *B.g. secalis*, presence/absence of genes was estimated by coverage analysis based on mappings of five re-sequenced isolates. Genes that are present in at least one *B.g. secalis* isolate, where considered as present. Genes and their orientation are indicated by triangles. The white rectangle in the *B.g. triticale* THUN-12 assembly indicates the position of the 50kb deletion presented in Fig. 1F. The gene marked with an asterisk represents a collapsed gene duplication in the *B.g. tritici* 96224 assembly that was resolved in the *B.g. triticale* THUN-12 genome assembly. Syntenic relationship is indicated by dashed lines. The figure is not drawn to scale. (C-E). The AvrPm17 gene copies have evolved through gene conversion. (C) Analysis of SNPs in the *AvrPm17* gene copies in the two parental isolates. SNPs in THUN-12 are shown in comparison to 96224 for which both gene copies are identical. The *AvrPm17* genes are represented schematically with grey boxes representing the two exons. The transcriptional orientation is indicated by the direction of the arrowhead in the second exon. SNPs are indicated in the coding sequences and the intron, as well as in regions 100bp up- and downstream of the gene. Red bars represent SNPs that are shared between the two gene copies in THUN-12 and yellow lines indicate SNPs that are present in only one copy. (D) Visual representation of the duplication of *AvrPm17* in isolate 96224. To allow alignment of the two sequences, the insertions in the downstream region of the two genes were spliced out. The x-axis shows the alignment position, while the y-axis shows the sequence identity calculated in 50bp sliding windows. The position of the *AvrPm17* gene is highlighted by a yellow box. (E) Dotplot

23

726   alignment of the duplicated gene copies and flanking region in the isolate THUN-12. Insertions in
727   the downstream region of BgTH12-04537 and BgTH12-04538 are highlighted in green and blue,
728   respectively.

729

Figure 4. Diversity analysis of AVRPM17 in different *formae speciales*. (A) Protein variants found in a global mildew population of 160 isolates (*B.g. tritici*, *B.g. triticale*, *B.g. dicocci*, *B.g. dactylidis*). Colors indicate differences in recognition strength determined by transient co-expression in *N. benthamiana*. Orange indicates the avirulence allele varA and haplotypes that are recognized to a comparable extent. Yellow indicates variants that are recognized significantly weaker than the avirulent allele *AvrPm17*_varA and therefore represent partial gain-of-virulence alleles. The only full loss-of-recognition variant is indicated in gray. (B) Distribution of haplotypes in global *B.g. tritici*, *B.g. triticale* and *B.g. dicocci* populations. (C) Recognition strength of AVRPM17 variants (depicted in panel (A)) in *N. benthamiana* compared to AVRPM17_varA. Infiltrations were performed at R: Avr ratios of R: Avr of 1:1 and significance was assessed using a paired Wilcoxon rank sum test, significance level are indicated above the boxplots as follows: **=p<0.05, *** p<0.01.

743

Figure 5. QTL mapping in the Bgt_96224 X THUN-12 F1 population on the wheat cultivar 'Amigo' carrying a 1RS.1AL translocation from 'Insave' rye including the *Pm17* resistance gene. (A) Representative photographs of phenotypes of the parental isolates Bgt_96224 and THUN-12 on Amigo at 10dpi. The susceptible wheat cultivar 'Kanzler' was used as an infection control. (B) Boxplot summarizing the phenotypes of Bgt_96224 and THUN-12 on 'Amigo'. Leaf coverage of individual leaf segments was scored according to the following scale: avirulent = 0, avirulent/intermediate 0.25, intermediate 0.5, intermediate/virulent =0.75, virulent = 0. (C) Distribution of phenotypes of the 117 progeny of the cross Bgt_96224 X THUN-12 on 'Amigo'. Progeny phenotypes were scored as described in (B) and the average of at least 6 leaf segments for each progeny was plotted (D) Single interval QTL mapping of Bgt_96224 X THUN-12 on cultivar 'Amigo'. The black line indicates the LOD (logarithm of the odds) score of the association throughout the 11 chromosomes of wheat powdery mildew. Red line indicates the significance threshold determined by 1000 permutations. (E) QTL effect plots summarizing phenotypes of the 117 progeny on 'Amigo'. The phenotypes were plotted based on the genotypes of the best associated marker at the QTL location on chromosome 9 (QTLchr09) and chromosome 1 (AvrPm17 locus). (E) Photographs of representative progeny of the cross Bgt_96224 X THUN-12 with different genotype combinations (see E) for the QTLs identified in (D). Phenotypes on wheat cultivar 'Amigo' and the transgenic lines expressing *Pm17* at 10dpi are shown.

26